Published in final edited form as:
Gut. 2014 November ; 63(11): 1769–1781. doi:10.1136/gutjnl-2013-306271.

Targeted depletion of a MDSC subset unmasks pancreatic ductal adenocarcinoma to adaptive immunity

Ingunn M. Stromnes[1,4], **Scott Brockenbrough**[1], **Kamel Izeradjene**[1], **Markus A. Carlson**[1], **Carlos Cuevas**[5], **Randi M. Simmons**[1], **Philip D. Greenberg**[1,3,4,*], and **Sunil R. Hingorani**[1,2,3,*]

[1]Clinical Research Division, Fred Hutchinson Cancer Research Center, Seattle, WA, 98109

[2]Public Health Sciences Division, Fred Hutchinson Cancer Research Center, Seattle, WA, 98109

[3]Department of Medicine, Division of Medical Oncology, University of Washington School of Medicine, Seattle, WA, 98195

[4]Department of Immunology, University of Washington, Seattle, WA, 98195

[5]Department of Radiology, University of Washington School of Medicine, Seattle, WA, 98195

Abstract

Objective—Pancreatic ductal adenocarcinoma (PDA) is characterized by a robust desmoplasia, including the notable accumulation of immunosuppressive cells that shield neoplastic cells from immune detection. Immune evasion may be further enhanced if the malignant cells fail to express high levels of antigens that are sufficiently immunogenic to engender an effector T cell response. In this report, we investigate the predominant subsets of immunosuppressive cancer-conditioned myeloid cells that chronicle and shape pancreas cancer progression. We show that selective depletion of one subset of myeloid-derived suppressor cells (MDSC) in an autochthonous, genetically engineered mouse model (GEMM) of PDA unmasks the ability of the adaptive immune response to engage and target tumor epithelial cells.

Methods—A combination of *in vivo* and *in vitro* studies were performed employing a GEMM that faithfully recapitulates the cardinal features of human PDA. The predominant cancer-conditioned myeloid cell subpopulation was specifically targeted *in vivo* and the biological outcomes determined.

Results—PDA orchestrates the induction of distinct subsets of cancer-associated myeloid cells through the production of factors known to influence myelopoeisis. These immature myeloid cells

[*]Correspondence: Sunil R. Hingorani, MD, PhD, Fred Hutchinson Cancer Research Center, Mail Stop M5-C800, P.O. Box 19024, Seattle, WA 98109-1024, srh@fhcrc.org, Philip D. Greenberg, MD, Fred Hutchinson Cancer Research Center, Mail Stop D3-100, P.O. Box 19024, Seattle, WA 98109-1024, pgreenberg@fhcrc.org.

Contributors
IMS, SB, KI, MAC, CC and RMS performed experiments; IMS, PDG and SRH designed the study and wrote the manuscript.

Competing Interests
None.

inhibit the proliferation and induce apoptosis of activated T cells. Targeted depletion of granulocytic MDSC (Gr-MDSC) in autochthonous PDA increases the intratumoral accumulation of activated CD8 T cells and apoptosis of tumor epithelial cells, and also remodels the tumor stroma.

Conclusions—Neoplastic ductal cells of the pancreas induce distinct myeloid cell subsets that promote tumor cell survival and accumulation. Targeted depletion of a single myeloid subset, the Gr-MDSC, can unmask an endogenous T cell response, revealing an unexpected latent immunity and invoking targeting of Gr-MDSC as a potential strategy to exploit for treating this highly lethal disease.

Keywords

Pancreatic Cancer; Immune Surveillance; Growth Factors

INTRODUCTION

Pancreatic ductal adenocarcinoma (PDA) is a highly lethal cancer with a rising incidence and unabated mortality.[3] PDA is associated with the highest 1-year and 5-year mortalities of any cancer, reflecting not only the ability to evade detection until advanced stages, but also an unusual proclivity for metastatic spread. Combined with the notorious resistance to conventional chemical and radiotherapies, the diagnosis of PDA inevitably portends a poor prognosis.

A robust fibroinflammatory reaction is essentially pathognomonic for PDA and renders tumor epithelial cells a minor component of the overall cellular mass.[4] The tumor stroma, comprised of inflammatory cells, pancreatic stellate cells, and endothelial cells embedded within a dense extracellular matrix (ECM), predominates in PDA and influences the response to therapy.[5, 6] Our previous work examined the content and kinetics of the immune reaction in a highly faithful GEMM of PDA.[7] An impressive immune presence at even the earliest stages of preinvasive disease could be identified, with a specific chronology of distinct immune subsets evolving during disease progression.[7] The unique temporal kinetics suggest that distinct immunosuppressive cells, accumulating from a very early time point, may mask tumor epithelial cells from immune detection at inception and invasion. Strategies that target specific immune cell subsets may therefore be required at each stage of cancer progression to surmount barriers to effective immunity.

An additional challenge to eliciting an endogenous T cell response may be a lack of sufficiently immunogenic antigens. Despite the widespread and complex genomic instability of PDA,[8] this disease appears to have few coding mutations.[9, 10] This can be contrasted with the mutational profiles of melanoma[11] and lung cancer,[12] malignancies that have been shown to respond to immunotherapies.[13, 14] The dependence on modulation of endogenous immunity in PDA may be more challenging due to what appears to be a rather limited neoantigenic spectrum. Indeed, similar immunomodulatory approaches in PDA have thus far exhibited limited but provocative clinical effects.[15–17] Thus, a better understanding of the impact of immunosuppressive cells on the recognition of PDA by the endogenous immune system is necessary for designing potentially useful immune-based therapies.

Recent studies have suggested that the establishment of transplanted preinvasive murine ductal epithelial cells[1] or of PDA allografts[2] could be inhibited by decreasing GM-CSF production in the transplant prior to implantation. The inhibition of tumor growth was reflected by a decrease in myeloid cells at the tumor site and was dependent on endogenous CD8 T cells.[2] However, since the grafts were comprised of cell lines from a heterologous (mixed) genetic background, or from cells virally transduced to exogenously express foreign proteins, the anti-tumor activity of endogenous CD8 T cells in this setting was likely due, at least in part, to recognition of minor histocompatibility allo-antigens or foreign epitopes. These findings are consistent with prior work demonstrating that MDSC can prevent graft rejection,[18–21] but leave unaddressed the potential therapeutic benefit of this strategy in a clinical oncology setting. Furthermore, it remains unclear if disrupting cancer-associated myeloid cells would have an impact on established, autochthonous pancreas cancers.

Here, we investigate the role of cancer-conditioned myeloid cells in a GEMM of autochthonous PDA, in which invasive disease arises *in situ* via the stochastic development and progression of ductal precursor lesions. As a consequence, the only antigens available for recognition by the endogenous immune system are naturally occurring tumor antigens. We find that two distinct subsets of MDSC, granulocytic (Gr-MDSC) and monocytic (Mo-MDSC), expand and chronicle PDA progression, and that selective targeting of Gr-MDSC is sufficient to induce the activation and proliferation of systemic and intratumoral CD8 T cells. The influx of activated CD8 T cells is associated with an increase in tumor epithelial cell apoptosis and remodeling of the stroma. These results suggest that depletion of MDSC is an attractive, if not essential, approach to potentiate classical cytotoxic and/or adoptive immunotherapy technologies, and may represent a critical component of a comprehensive platform to treat this formidable disease.

MATERIALS AND METHODS

Mouse Strains

All animal studies were approved by the Institutional Animal Care and Use Committee of Fred Hutchinson Cancer Research Center. The *Kras*$^{LSL\text{-}G12D/+}$*;Cre* (*KC*)[22] and *Kras*$^{LSL\text{-}G12D/+}$*;Trp53*$^{LSL\text{-}R172H/+}$*;Cre* (*KPC*)[23] genetically engineered models of PDA have been previously described.

Isolation of mononuclear cells from tissues

Pancreatic lymph nodes were removed from primary PDAs using a dissecting microscope prior to digestion of tumors with collagenase (SIGMA-Aldrich C2674, 1 mg/ml in DMEM/F12) for 30 min at 37°C in a rotating incubator. Cells were washed in DMEM/F12/10% FBS prior to cell counting and staining. Erythrocytes were lysed from blood, spleen and bone marrow mononuclear preparations using ACK Lysing Buffer (Life Technologies). Single cell suspensions were established in DMEM/F12/10% FBS for analyses.

Immune profiling and sorting

Mononuclear cells isolated from the spleens and tumors of *KPC* mice were incubated with fluorescently conjugated monoclonal antibodies as follows: CD45 (Ly5 1:200), CD11b

(M1/70 1:200), Gr-1 (RB6-8C5 1:200), Ly6C (HK1.4 1:200), Ly6G (1A8 1:200), CD8α (53-6.7 1:200), CD69 (R1-2 1:100), CD25 (PC61 1:100), and Ki67 (B56 1:100) (BD Biosciences). Intracellular staining for Ki67 was performed using the eBioscience Foxp3/ Transcription Factor Staining Buffer Set. Annexin-V (BD Biosciences) staining was performed according to the manufacturer's recommendations. Flow cytometric analysis of immune cells was performed by gating on live $CD45^+$ cells using a BD Biosciences FACSCanto II. $CD45^+CD11b^+Gr\text{-}1^{high}$ $Ly6C^{int}$ cells were purified from the bone marrow, spleen and tumor of *KPC* mice with invasive PDA by cell sorting using a BD Biosciences FACSAria II to >90% purity.

Histopathology and immunofluorescence

For histopathological analysis, tissues were fixed in 10% formalin for 96h, embedded in paraffin, and 4–5 μ sections were stained with H&E, Masson's trichrome or Movat's pentachrome. For immunofluorescence, OCT tissue sections (7 μ) were fixed in acetone at −20°C, blocked with PBS/1% BSA and incubated with the following primary antibodies: cleaved caspase-3 (Cell Signaling D175, 1:200), CD8α (BD Biosciences 53-6.7, 1:25), Gr-1 (eBioScience RB6-8C5, 1:50), Ly6G (Bioxcell 1A8, 1:50), PanCK-FITC (SIGMA-Aldrich F3418, 1:200), SMA-1 (DAKO 1A4, 1:100), CD31 (BD Biosciences 390, 1:50) or granzyme B (R&D Systems, 1:50). Sections were washed with PBS/1% BSA, labeled with species specific Alexa-conjugated antibodies (Invitrogen) and washed with PBS/1% BSA followed by PBS. The sections were mounted using Prolong gold anti-fade reagent with DAPI to label nuclei (Invitrogen).

T cell suppression assay

To measure CD8 T cell proliferation, 96-well round-bottom plates were pre-coated with 100 μl anti-CD3ε (BD Biosciences 145-2C11, 1 μg/ml) and anti-CD28 (BD Biosciences 37.51, 10 μg/ml) and incubated at 4°C for 24h. Splenic CD8 T cells were purified using Dynabeads Untouched Mouse CD8 Cell isolation kit (Invitrogen) according to the manufacturer's protocol. Purified CD8 T cells were labeled with 1 μM 5,6-carboxyfluorescein diacetate succinimidyl ester (CFSE, Invitrogen) at 37°C for 20 min in serum-free RPMI. Excess dye was removed by washing the labeled cells with RPMI 1640 supplemented with 2 μM glutamine, 100 U/ml penicillin/streptomycin, 10% fetal calf serum and 30 μM 2-mercapatoethanol (complete media). Sorted Gr-MDSC ($CD45^+CD11b^+$ $Gr\text{-}1^{high}LyC^{int}$), Mo-MDSC ($CD45^+CD11b^+Gr\text{-}1^{int}Ly6C^{high}$) or TAM ($CD45^+CD11b^+Gr\text{-}1^{int}Ly6C^{int}$) were incubated at titrating numbers with 1×10^5 CFSE-labeled labeled T cells in complete media. After 48h, cell cultures were stained for surface markers with CD8α-e450 (BD Biosciences 53-6.7, 1:200) and Thy1.1 (CD90.1)-PercP (BD Biosciences OX-7, 1:200) in PBS/2.5% FBS, followed by Annexin-V-APC (BD Biosciences) staining according to the manufacturer's protocol, and immediately analyzed on a FACSCanto II. The percentages of apoptotic (Annexin-V) or proliferating (CFSE-dilution) T cells were determined by gating on $CD8^+$ $Thy1.1^+$ cells.

Proteome analysis

Conditioned media (CM) isolated from 24h supernatants of purified preinvasive (n=2), invasive (n=2) and paired metastatic (n=2) *KPC* carcinoma cells were incubated on Mouse Cytokine Array Panel A nitrocellulose membranes (R&D Systems ARY006) according to manufacturer's recommendations. The mean pixel density for each capture antibody spot in duplicate was calculated and proteins that were positive in ≥ 2 independent invasive cell preparations were quantified by real-time PCR.

Gene expression analysis

Total RNA was extracted (RNeasy Miniprep Kit, Qiagen) from primary cultures of *KPC* tumor epithelial cells and paired metastatic cells to the livers of the same animals (n=3 each), and also from preinvasive pancreatic ductal epithelial cells. RNA was converted to cDNA using a High Capacity Reverse Transcriptase Kit (Applied Biosystems). Quantitative PCR was performed using SYBR Green mastermix and triplicate samples were run on a C1000 Thermal Cycler (BioRad). Primers (supplementary table 1) were based on published literature or designed using Primer-BLAST software. Quantifications were normalized to endogenous *cycA* and fold-change gene expression in invasive and metastatic cells compared to preinvasive cells was calculated using the ΔΔCT method.

MDSC depletion

KPC mice were serially imaged by high-resolution ultrasound (Vevo 2100, Visualsonics) and enrolled when the primary tumor reached 2–5 mm in diameter. The monoclonal antibody (mAb) 1A8 (Bioxcell, 400 μg in sterile saline) was administered i.p. on days 0, 5 and 10 to deplete $Ly6G^+$ Gr-MDSC. Control *KPC* mice were treated with saline or isotype (Rat IgG2a) control. For immunomodulation experiments, tumor diameters were assessed in a blinded manner by high-resolution ultrasound at time of enrollment, and on days 8 and 12 of treatment.

MDSC Proliferation and Apoptosis Assays

$CD11b^+Gr\text{-}1^{high}$ $Ly6C^{int}$ MDSC were isolated to >90% purity and incubated with 1 μM CFSE (Invitrogen) at 37°C for 20 min in serum-free media. Excess dye was removed by washing labeled cells with complete media. A total of 1×10^5 Gr-MDSC were incubated with basic media (DMEM/F12/10% FBS) or with CM isolated from the supernatants of primary PDA cells (PDA-CM) or metastatic PDA cells (Met-CM); the recombinant murine cytokines, GM-CSF, G-CSF, or M-CSF (R&D Systems, 50 ng/ml); or blocking antibodies to GM-CSF, G-CSF, or M-CSF (R&D Systems, 10 μg/ml). After 48h, cells were stained for Gr-1-e450 (BD Biosciences RB6-8C5, 1:200) and CD11b-PE (BD Biosciences M1/70, 1:200), and Annexin-V-APC and CFSE dilution were measured by gating on live $Gr\text{-}1^+CD11b^+$ cells to assess for apoptosis and proliferation, respectively.

Quantification of vessel diameter in tumors

Frozen sections were dual stained with anti-mouse CD31 (BD Biosciences 390, 1:50) followed by species-specific Alexa-conjugated secondary antibody (Invitrogen, 1:1000) and PanCK-FITC (SIGMA-Aldrich F3418, 1:200). Vessel diameters were measured using NIS-

Element imaging software from 3–5 non-overlapping 20× fields in PDA sections from control and mAb 1A8-treated *KPC* mice (n=3 animals each). Typically between 5–10 vessels were measured per high-powered field.

Statistical analyses

Analyses were performed with Prism Graphpad software. Data are provided as mean ± SEM, unless indicated otherwise. For comparisons between two groups, statistical analyses were performed using a Student's t-test and $p<0.05$ was considered significant. For comparisons involving 3 groups or more, a one-way ANOVA using the Kruskal-Wallis test was first performed ($p<0.05$ was considered significant), followed by a Dunn's Multiple Comparison Test (unless otherwise indicated). Symbols indicating statistical significance are as follows: *, $p<0.05$; **, $p<0.005$; ***, $p<0.0005$.

RESULTS

Systemic and intratumoral accumulation of myeloid cells chronicles PDA progression

Targeted endogenous expression of oncogenic $Kras^{G12D}$ and point mutant $Trp53^{R172H}$ to progenitor cells of the murine pancreas[23] induces the development of a clinical, histopathologic and molecular syndrome of disease that faithfully recapitulates human PDA.[24] Disease initiates in preinvasive ductal precursors, termed pancreatic intraepithelial neoplasias (PanINs), and progresses spontaneously to invasive and metastatic ductal adenocarcinoma. As described previously in *KC* mice,[7] we found that discrete immune cell populations infiltrate at distinct stages in evolving *KPC* PDA. $CD4^+$ $Foxp3^+$ regulatory T cells (Treg) and tumor associated macrophages (TAM) infiltrated predominantly at the preinvasive stage, while Gr-1^+ $CD11b^+$ cells increased most markedly in the transition from preinvasive to invasive disease (figure 1A).

Since Gr-1^+ cells increased precipitously from preinvasive to invasive disease to become a dominant immune cell population infiltrating PDA, we sought to further clarify the nature of these cells during malignant progression. The monoclonal antibody (mAb) RB6-8C5 was initially described to bind to granulocyte receptor 1 (Gr-1), historically synonymous with Ly6G.[25] It is now clear, however, that RB6-8C5 binds to two distinct cell surface antigens: Ly6G, which is specifically expressed on granulocytes, and Ly6C which is expressed on a variety of cells types including $CD11b^+$ inflammatory monocytes,[26] plasmacytoid dendritic cells,[27, 28] and $CD8^+$ T cells.[29] Therefore, to distinguish potentially distinct cancer-conditioned myeloid cell populations, we used three different reagents: mAb αGr-1 (clone RB6-8C5), which binds both Ly6G and Ly6C; mAb αLy6G (clone 1A8); and mAb αLy6C (clone HK1.4). Of relevance, $CD11b^+$ inflammatory monocytes in normal mice (also referred to as Mo-MDSC in tumor-bearing mice) bind RB6-8C5 due to high levels of Ly6C expression, but do not express Ly6G.[30] The predominant subset of CD11b myeloid cells that were induced systemically stained brightly with RB6-8C5 (Gr-1^{high}) and expressed intermediate levels of Ly6C (Ly6C^{int}), and these $CD11b^+$Gr-1^{high} Ly6C^{int} cells are hereafter referred to as Gr-MDSC (figure 1B). As expected, Gr-1^{high} cells also stained positively for Ly6G as detected by mAb 1A8, while other $CD11b^+$ myeloid subsets, including Gr-1^{int} Ly6C^{high} cells did not express Ly6G (data not shown). Significant increases in the

percentage of Gr-MDSC in bone marrow (p=0.0036), blood (p=0.0033), spleen (p=0.0238), and pancreas (p=0.0167) were observed in mice with PDA compared to control littermates. Furthermore, Gr-MDSC were rarely detected in pancreatic draining lymph nodes (dLN) from non-tumor bearing mice, but were increased in dLN associated with PDA (figure 1B, supplementary figure 1). The absolute number of Gr-MDSC was significantly higher in the spleens and primary tumors of mice that had progressed to invasive disease as compared to *KPC* mice with preinvasive disease only (figure 1C). The absolute number of Mo-MDSC ($CD11b^+$ $Gr\text{-}1^{int}$ $Ly6C^{high}$) increased significantly in the spleens of mice with invasive PDA as compared to mice with preinvasive disease only, but this population was not significantly increased within the autochthonous tumor itself (figure 1C). The marked rise in Gr-MDSC and Mo-MDSC in the circulation during disease progression also correlated with a reduction in the percentage, though not absolute number, of $Gr\text{-}1^{neg/low}$ $F4/80^+$ cells within the CD11b compartment in the spleen, likely reflecting dilution from extramedullary hematopoiesis and associated splenomegaly. $CD11b^+$ $Ly6C^{int}$ $F4/80^+$ $Ly6G^-$ cells were common in PDA, stained positive for RB6-8C5 due to Ly6C expression, and were adherent *in vitro* (not shown), further distinguishing them from the two MDSC subpopulations.

The localization of Gr-MDSC within the pancreas during disease evolution was determined by dual immunofluorescence for ductal epithelial cells (Pan-CK) and for myeloid populations using 1A8, which specifically detects Gr-MDSC and not Mo-MDSC, or RB6-8C5, which detects both of these populations and TAM as well. Immunoreactivity with RB6-8C5 was observed on a small fraction of cells in the normal pancreas, and notably in rings of cells encircling PanINs, identifying tissue resident $Ly6C^+$ macrophages (note that these cells are not identified by 1A8) (figure 1D).[31] RB6-8C5 staining was also detected in a small fraction of cells in the normal salivary gland (figure 1E). In contrast, there were scant Gr-MDSC (as determined by 1A8 reactivity) in the normal pancreas and only a modest infiltration in pancreata with preinvasive lesions. $Ly6G^+$ Gr-MDSC were abundant and widely dispersed throughout invasive PDA, consistent with the flow cytometry data (figure 1D).

Distinct morphological spectra distinguish MDSC subsets

The nuclear morphology of phenotypic Gr-MDSC revealed cells with segmented nuclei, consistent with polymorphonuclear cells (PMN),[32] as well as more immature forms that had ring or horseshoe shaped nuclei indicative of immature myeloid progenitors (so-called “band” cells; supplementary figures 2A, B). Phenotypic Mo-MDSC isolated from the spleen contained these immature forms as well as monocytes, but segmented cells were rarely detected (supplementary figure 2A). Although ring cells were identified in both subsets, these cells have been suggested to be functionally distinct, as $Gr\text{-}1^{high}$ ring cells include mature cells of the granulocyte lineage, while $Gr\text{-}1^{low}$ ring cells include a more heterogeneous mononuclear population.[33] Gr-MDSC also exhibited higher side-scatter by FACS analyses, reflecting increased granularity as compared to Mo-MDSC, and were more uniform in size as compared to the Mo-MDSC population (supplementary figures 2A, B). Splenic and intratumoral Gr-MDSC expressed the differentiation markers F4/80 and MHC class II, which were not detected on PMN isolated from normal mice (data not shown). The presence of these additional markers was restricted to Gr-MDSC isolated from the spleen

and tumors, and not found on $CD11b^{+}Gr\text{-}1^{high}$ cells in the blood or bone marrow of animals with PDA (supplementary figure 2C), suggesting evolution through additional maturation stages from marrow to periphery during malignancy. The fact that tumor-associated Gr-MDSC can express F4/80 and MHC class II molecules also indicates that some of these markers in malignancy are imprecise and may fail to clearly distinguish macrophages from MDSC.

Gr-MDSC inhibit T cell proliferation and induce T cell death after activation

Pooled $Gr\text{-}1^{+}$ cells from tumor-bearing mice, which contain both the monocytic and granulocytic subsets, have been shown to suppress T cell proliferation.[2, 7] To determine the suppressive potential of each of these subpopulations, sorted Gr-MDSC ($CD11b^{+}$ $Gr\text{-}1^{high}$ $Ly6C^{int}$), Mo-MDSC ($CD11b^{+}$ $Gr\text{-}1^{int}$ $Ly6C^{high}$), and TAM ($CD11b^{+}$ $Gr\text{-}1^{int}$ $Ly6C^{int}$) from *KPC* mice were incubated with T cells in both proliferation and apoptosis assays. At a 1:1 myeloid-to-T cell ratio, Gr-MDSC moderately decreased naïve T cell proliferation (figure 2A). However, at the higher myeloid-to-T cell ratios observed *in vivo* in mice with PDA, Gr-MDSC exhibited a pronounced ability to suppress T cell proliferation and the degree of suppression was dose-dependent (figure 2B). Mo-MDSC also significantly suppressed T cell proliferation in a dose-dependent manner and TAM potently blocked T cell cycling (supplementary figure 3).

Gr-MDSC, Mo-MDSC and TAM also induced apoptosis of activated T cells (figures 2C, D and supplementary figure 3). Gr-MDSC isolated from PDA were 1.5-fold more potent at inducing T cell apoptosis than their splenic or bone marrow counterparts (figures 2C, D and data not shown). Thus, Gr-MDSC can both suppress T cell proliferation and promote T cell death, and the tissue milieu from which these cells are recovered appears to influence their immunosuppressive capacities. Since Gr-MDSC undergo the most dramatic and significant increase in number from preinvasive to invasive PDA, we chose to study this subset in more detail.

Tumor conditioned media and GM-CSF promote Gr-MDSC survival

We observed that neither splenic nor tumor-derived Gr-MDSC survived after 24h of culture in standard media as indicated by the collapse of cellular integrity and the appearance of pyknotic nuclei and cell debris (figure 3A). This was in clear contrast to the abundant, large, viable, birefringent Gr-MDSC clusters in media that had been conditioned by either primary or metastatic PDA cells (figure 3A and data not shown). Conditioned media (CM) from cultured PDA cells prevented the majority of Gr-MDSC from undergoing apoptosis (figure 3B).

To investigate the molecular mechanisms underlying the enhanced survival of Gr-MDSC in response to conditioned media, we profiled the soluble factors expressed by purified carcinoma cells in culture. The secretory profile of invasive and metastatic cells revealed a substantial commitment to synthesis of growth factors and chemokines involved in both granulocyte (*e.g.*, CXCL1, CXCL2) and monocyte (*e.g.*, CCL2) trafficking (supplementary figure 4). Granulocyte macrophage colony stimulating factor (GM-CSF), granulocyte colony stimulating factor (G-CSF), and monocyte colony stimulating factor (M-CSF) were also

upregulated in tumor epithelial cells as compared to preinvasive ductal cells. Relative gene expression by quantitative PCR confirmed the increase in these factors in invasive versus preinvasive cells (figure 3C). Of these three myelopoietic cytokines,[34] GM-CSF had the most pronounced effect on promoting Gr-MDSC survival *in vitro* (figures 3D, E). Furthermore, blockade of GM-CSF in CM significantly decreased the percentage of live (non-apoptotic) Gr-MDSC (figure 3F), implicating GM-CSF as a primary tumor cell secreted factor promoting Gr-MDSC survival. Of note, G-CSF produced by PDA also consistently increased Gr-MDSC survival (figures 3D–F). However, neither conditioned media nor these cytokines were sufficient to promote appreciably the proliferation of Gr-MDSC *in vitro* (not shown), suggesting either that additional factors sustain MDSC proliferation *in vivo* or accumulation is instead due to the prevention of apoptosis and/or the induction or expansion of precursors. The chemokines CXCL1, CXCL2 and CCL2 had no impact on Gr-MDSC survival or proliferation *in vitro* (data not shown). Finally, we confirmed that preinvasive and invasive PDA epithelial cells secrete GM-CSF *in vivo* and note that GM-CSF-containing vesicles within the cells are orientated toward the parenchyma rather than the lumen of duct-like structures (figure 3F). These data support a model in which primary tumor epithelial cells secrete factors into their microenvironment that promote the survival and recruitment of Gr-MDSC, contributing to their *in vivo* accumulation during cancer progression.

Depletion of Gr-MDSC increases CD8 T cell accumulation and activation in autochthonous PDA

In order to investigate the clinical potential of targeting MDSC, we performed experiments to deplete MDSC in animals with autochthonous invasive and metastatic PDA. *KPC* mice with a defined primary pancreatic tumor burden of 2–5 mm in diameter by high resolution ultrasound were injected with the αLy6G mAb 1A8[35] to deplete the Gr-MDSC, while not reducing the number of $Ly6G^-$ Mo-MDSC (figures 4A, B and data not shown). We developed and refined our treatment protocol to maintain effective depletion of intratumoral Gr-MDSC for over 2 weeks. We also established the ability of RB6-8C5 to deplete MDSC (data not shown); however, since this antibody has been shown to induce signaling,[36] and is also less specific, we focused on 1A8 for the more detailed studies presented here. Administration of 1A8 markedly reduced the percentage and number of Gr-MDSC not only in the circulation (figures 4A, B), but also in the spleen (figures 4C, D) and PDA (figures 4E, F). Intriguingly, a corresponding 4 – 5-fold increase was seen in the number of Mo-MDSC in the spleen ($1.4 \pm 0.24 \times 10^7$ control vs. $6.3 \pm 1.9 \times 10^7$ in 1A8-treated, p=0.0019) and PDA of 1A8-treated mice ($5.0 \pm 1.1 \times 10^6$ control vs. $2.6 \pm 0.52 \times 10^7$ in 1A8-treated, p<0.0001), suggesting a homeostatic relationship between these two myeloid subpopulations. Tumor masses did not generally decrease in size during this treatment window and, in the majority of 1A8-treated mice, the tumors instead grew (not shown). Although this could be interpreted to reflect a lack of efficacy, immune therapies have frequently been shown to cause acute increases in tumor size due to the recruitment and infiltration of immune cells, rather than the progressive growth of the cancer cells.[37] Consistent with this possibility, the number of intratumoral $CD45^+$ immune cells in 1A8-treated mice increased ~2-fold compared with untreated PDA, although this did not reach

statistical significance ($1.04 \pm 0.16 \times 10^7$ in controls vs. $2.4 \pm 0.9 \times 10^7$ in 1A8-treated mice; n=4 each; p=0.1557).

The influx of immune cells in Gr-MDSC-depleted animals prompted us to examine the composition of the infiltrate in greater detail and to analyze additional cellular and molecular endpoints. Depletion of Gr-MDSC significantly increased the percentage and absolute number of CD8 T cells in autochthonous PDA (figures 5A, B), as well as the fraction that were proliferating (figures 5C, D). Consistent with this proliferative signature, a higher proportion of CD8 T cells in the spleen and invasive PDA expressed the activation marker CD69, indicative of antigen recognition and signaling by the T cell receptor[38, 39] (figures 5E, F). CD8 T cell accumulation in PDA after Gr-MDSC depletion was also detected *in situ* by specific immunofluorescence (figure 5G). Tumor-infiltrating CD8 T cells were found not only in the stroma, but also immediately adjacent to tumor epithelial cells (figure 5G). Cytokeratin staining was more punctate and less uniform in areas adjacent to CD8 T cells as compared to immune-privileged tumor areas, suggesting a potential effect on epithelial cell integrity (and see below). An additional indication of T cell activation is transient release of the serine protease granzyme B that can be captured in a subset of cells at any given point in time. The number of granzyme B+ cells was significantly increased in Gr-MDSC-depleted mice (supplementary figures 5A, B). Thus, Gr-MDSC depletion also impacts the functional activity of tumor-infiltrating T cells.

Depletion of Gr-MDSC increases tumor epithelial apoptosis in autochthonous PDA

Standard histological and histochemical studies immediately revealed that targeted depletion of Gr-MDSC had influenced the stromal architecture and integrity of the tumors in treated mice, particularly in regions with concentrated mononuclear cells (figure 6). These areas were also characterized by decreased ECM deposition and the appearance of patent blood vessels (figure 6A), with increased vessel diameters (figure 6B, C), which are otherwise typically compressed and not readily visible in PDA.[5, 6] Depletion of Gr-MDSC also resulted in a 3-fold increase in cleaved caspase-3 (CC3)-positive tumor cells, but did not change the number of proliferating cells (figure 6D). Compound immunofluorescence assays confirmed that a significant fraction of apoptotic cells represented tumor epithelium (figure 6D). Apoptosis was not appreciably increased in activated myofibroblasts (supplementary figure 5C). Taken together, these results support the hypothesis that cancer-conditioned Gr-MDSC may impede the recognition of tumor antigens by CD8 T cells and the acquisition of effector T cell activity in PDA, and that targeted depletion of Gr-MDSC with systemic mAb therapy can potentially unmask PDA to endogenous immunity.

DISCUSSION

Cancer implies a failure of immunity. Indeed, in cancers like PDA, it may even suggest immune complicity. Preinvasive cells can persist in the context of a fully functional immune system for manifold reasons. Since tumors are derived from self, they benefit from multiple mechanisms of self-tolerance. Common driver mutations in cancer cells may not encode strongly immunogenic epitopes, and malignant cells are notoriously defective in antigen processing and presentation, which further contribute to immune evasion.[40] Neoplastic cells

have additional elaborate mechanisms that subvert anti-tumor T cell activity, including the induction of host immunosuppressive cells. Although endogenous tumor-reactive T cells can, in principle, recognize cancer antigens expressed on preinvasive cells and delay malignant progression,[41] concomitant induction of T cell tolerance can abrogate expression of an effector response.[42]

This study is the first to report that depletion of a single immunosuppressive myeloid cell subset can induce endogenous CD8 T cell accumulation and tumor cell death in autochthonous ductal adenocarcinomas of the pancreas. That adaptive immunity appears to be induced without providing additional signals to positively engage an antigen-specific T cell response is especially surprising in PDA, which has seemed to be less immunogenic than other cancers.[9] Our data demonstrate that the endogenous immune response does have some capacity to recognize native PDA antigens and that Gr-MDSC present a critical barrier to eliciting such immune activity. Furthermore, in contrast to the hypothesis that intratumoral fluid pressure (IFP) and subsequent vessel compression (which we have shown can inhibit passive transport of molecules into PDA),[6] also limits immune cell infiltration,[43] our data indicate that T cells are readily capable of infiltrating tumors, as would be expected for cells which can employ active, ATP-dependent mechanisms to overcome passive barriers.

MDSC are induced in a variety of pathological settings, and have even been shown to prevent allograft rejection.[18–21] A recent study showed that inhibiting GM-CSF production by tumor cells reduced MDSC and inhibited the ability to establish PDA-derived allografts.[2] It is difficult, however, to draw definitive conclusions about PDA immunobiology from transplantable tumors, particularly allografts differing in histocompatibility antigens. Moreover, those studies did not distinguish among MDSC subpopulations. As shown here, depletion of Gr-MDSC in advanced stages of invasive autochthonous PDA is sufficient to induce epithelial tumor cell apoptosis and stromal remodeling. Our observation of increased systemic activation of CD8 T cells in this setting further supports the hypothesis that Gr-MDSC may limit the priming and/or boosting of tumor-reactive T cells in secondary lymphoid organs. Additionally, intratumoral MDSC may limit T cell accumulation in PDA by inducing apoptosis of the tumor-infiltrating T cells.

The remodeling of the stroma was an unexpected consequence of Gr-MDSC depletion and may result from the killing of tumor epithelial cells by activated T cells. Tumor epithelial cells can contribute to stromal architecture and composition through the direct secretion of ECM components and via paracrine signaling to myofibroblasts.[44] Although not our primary intent when investigating immunomodulatory strategies to render PDA more permissive to T cell activity, Gr-MDSC depletion may have the added benefit of improving chemotherapy access into tumors by increasing tumor vessel diameters, reminiscent of our findings with hyaluronidase.[6] However, combining immunomodulatory strategies to stimulate T cell function with cytotoxic agents could be challenging and even counterproductive, as the latter may undo the effects of the former by killing newly proliferative T cells.

The targeted depletion of Gr-MDSC was associated with a corresponding increase in a monocytic subset (Mo-MDSC) with comparable *in vitro* suppressive activity. It is somewhat

surprising therefore that endogenous T cells are activated and infiltrate PDA despite the compensatory rise in Mo-MDSC. Mo-MDSC may be unable to substitute fully for Gr-MDSC to confer an equivalent immunosuppressive environment *in vivo*; however, it is also possible that targeted depletion of Gr-MDSC provides a window of opportunity to induce an activated CD8 T cell response.

The human corollary of the murine Gr-MDSC described here are the $CD11b^{+}$ $CD33^{int}$ $Lin^{-/low}$ cells that are elevated in patients with PDA.[45–47] Additionally, the granulocytic markers CD15 and CD66b have also been used to define Gr-MDSC in human malignancies.[47–49] Thus, targeting this subpopulation of cells may therefore be an attractive therapeutic strategy. Some caution with this approach is warranted, however, as the monocytic subset of MDSC ($CD11b^{+}$ $CD33^{high}$ $CD14^{+/dull}$ $HLA\text{-}DR^{neg/low}$) has also been defined in a variety of human malignancies[45, 46, 50] and we have shown here that targeting Gr-MDSC can induce a corresponding expansion of Mo-MDSC. A recent study found that the percentage of circulating inflammatory monocytes, which share many of the same markers as Mo-MDSC in both mice and humans, correlated with a higher incidence of lymph node metastasis in patients with PDA and inversely with patient survival.[51] Therefore, additional studies are necessary to elucidate the ideal approach to modulate the highly plastic and interdependent cancer-conditioned myeloid cell subsets, and the success of such strategies may be cancer subtype-specific.

A number of mechanisms may be exploited to disrupt the immunosuppressive capability of Gr-MDSC including targeting their induction from progenitor cells, preventing trafficking into tumors, preventing their accumulation, inhibiting their immunosuppressive activity, or inducing their maturation (e.g. into cells that promote T cell activation).[52] Since the phenotypically defined myeloid subsets may reflect a continuum of cellular differentiation governed by homeostatic regulation, it may be possible to shift the respective balance to advantage. As an example, vaccination in combination with the administration of all-trans-retinoic acid (ATRA), which can have both immunogenic and inhibitory effects including inducing immature myeloid cells to differentiate into mature dendritic cells, was shown to promote the development of functional tumor antigen-specific T cells in small cell lung cancer patients.[53]

That tumor-produced GM-CSF and G-CSF may figure prominently in the induction and survival of MDSC suggests that a reassessment of the use of this cytokine as part of cancer treatment may be warranted. Providing growth factor support is common in oncology practice as a means of restoring or bolstering hematopoiesis in patients receiving cytotoxic chemotherapies.[54] Some of these agents are also used as adjuvants in many anti-tumor vaccine strategies.[17] Of course, growth factors can themselves exert pleiotropic effects on immunity and tumor biology and these effects depend both on the specific complement of cells in question and the stage of disease progression. The potential role of GM-CSF in facilitating the invasive and metastatic program in PDA suggests that it may be prudent to revisit its use in at least certain cancer treatment settings.

The limitations encountered thus far in applying immunomodulatory strategies such as αCTLA4 and αPD1/PDL1 in PDA to stimulate an endogenous T cell response may be the

result of the profoundly suppressive effects of MDSC. Combining targeted disruption of MDSC with additional immune-based strategies may help harness the full potential of the immune system to recognize and eradicate malignancies. Adoptive T cell technologies employed with a platform to abrogate MDSC function may prove especially potent in PDA and other solid tumors.

Supplementary Material

Refer to Web version on PubMed Central for supplementary material.

Acknowledgments

We thank members of FHCRC Comparative Medicine and Experimental Histopathology Shared Resources for expert assistance, Paolo Provenzano for assistance with analyzing expression data, Michael Ports for help with preliminary experiments, Ashley Dotson for assistance with animal husbandry and care, and Shelley Thorsen for expert assistance with manuscript and figure preparation.

Funding

This work was supported by the National Cancer Institute grants CA161112 and CA114028 to S.R.H., and support to S.R.H. from the Giles W. and Elise G. Mead Foundation and the Safeway Foundation, National Cancer Institute grant CA033084 to P.D.G, and the Fred Hutchinson Cancer Research Center/University of Washington Cancer Consortium Cancer Center Support Grant CA015704 (to P.D.G. and S.R.H.). The Irvington Institute Fellowship Program of the Cancer Research Institute and the Jack Paul Estate Fund to Support Collaborative Immunotherapy Research provided support for I.M.S.

REFERENCES

1. Pylayeva-Gupta Y, Lee KE, Hajdu CH, et al. Oncogenic Kras-induced GM-CSF production promotes the development of pancreatic neoplasia. Cancer cell. 2012; 21:836–847. [PubMed: 22698407]
2. Bayne LJ, Beatty GL, Jhala N, et al. Tumor-derived granulocyte-macrophage colony-stimulating factor regulates myeloid inflammation and T cell immunity in pancreatic cancer. Cancer cell. 2012; 21:822–835. [PubMed: 22698406]
3. Siegel R, Naishadham D, Jemal A. Cancer statistics, 2012. CA: a cancer journal for clinicians. 2012; 62:10–29. [PubMed: 22237781]
4. Hruban, R. Tumors of the pancreas. Hruban, RH.; Pitman, MB.; Klimstra, DS., editors. 2007.
5. Olive KP, Jacobetz MA, Davidson CJ, et al. Inhibition of Hedgehog signaling enhances delivery of chemotherapy in a mouse model of pancreatic cancer. Science. 2009; 324:1457–1461. [PubMed: 19460966]
6. Provenzano PP, Cuevas C, Chang AE, et al. Enzymatic targeting of the stroma ablates physical barriers to treatment of pancreatic ductal adenocarcinoma. Cancer cell. 2012; 21:418–429. [PubMed: 22439937]
7. Clark CE, Hingorani SR, Mick R, et al. Dynamics of the immune reaction to pancreatic cancer from inception to invasion. Cancer Res. 2007; 67:9518–9527. [PubMed: 17909062]
8. Campbell PJ, Yachida S, Mudie LJ, et al. The patterns and dynamics of genomic instability in metastatic pancreatic cancer. Nature. 2010; 467:1109–1113. [PubMed: 20981101]
9. Biankin AV, Waddell N, Kassahn KS, et al. Pancreatic cancer genomes reveal aberrations in axon guidance pathway genes. Nature. 2012; 491:399–405. [PubMed: 23103869]
10. Vogelstein B, Papadopoulos N, Velculescu VE, et al. Cancer genome landscapes. Science. 2013; 339:1546–1558. [PubMed: 23539594]
11. Cifola I, Pietrelli A, Consolandi C, et al. Comprehensive genomic characterization of cutaneous malignant melanoma cell lines derived from metastatic lesions by whole-exome sequencing and SNP array profiling. PloS one. 2013; 8:e63597. [PubMed: 23704925]

12. Govindan R, Ding L, Griffith M, et al. Genomic landscape of non-small cell lung cancer in smokers and never-smokers. Cell. 2012; 150:1121–1134. [PubMed: 22980976]
13. Lipson EJ, Drake CG. Ipilimumab: an anti-CTLA-4 antibody for metastatic melanoma. Clinical cancer research : an official journal of the American Association for Cancer Research. 2011; 17:6958–6962. [PubMed: 21900389]
14. Topalian SL, Hodi FS, Brahmer JR, et al. Safety, activity, and immune correlates of anti-PD-1 antibody in cancer. The New England journal of medicine. 2012; 366:2443–2454. [PubMed: 22658127]
15. Royal RE, Levy C, Turner K, et al. Phase 2 trial of single agent Ipilimumab (anti-CTLA-4) for locally advanced or metastatic pancreatic adenocarcinoma. Journal of immunotherapy. 2010; 33:828–833. [PubMed: 20842054]
16. Brahmer JR, Tykodi SS, Chow LQ, et al. Safety and activity of anti-PD-L1 antibody in patients with advanced cancer. The New England journal of medicine. 2012; 366:2455–2465. [PubMed: 22658128]
17. Strimpakos AS, Syrigos KN, Saif MW. Novel agents in early phase clinical studies on refractory pancreatic cancer. JOP : Journal of the pancreas. 2012; 13:166–168. [PubMed: 22406592]
18. Zhang W, Liang S, Wu J, et al. Human inhibitory receptor immunoglobulin-like transcript 2 amplifies CD11b+Gr1+ myeloid-derived suppressor cells that promote long-term survival of allografts. Transplantation. 2008; 86:1125–1134. [PubMed: 18946352]
19. Adeegbe D, Serafini P, Bronte V, et al. In vivo induction of myeloid suppressor cells and CD4(+)Foxp3(+) T regulatory cells prolongs skin allograft survival in mice. Cell transplantation. 2011; 20:941–954. [PubMed: 21054938]
20. Chou HS, Hsieh CC, Yang HR, et al. Hepatic stellate cells regulate immune response by way of induction of myeloid suppressor cells in mice. Hepatology. 2011; 53:1007–1019. [PubMed: 21374665]
21. Wang Y, Gu X, Xiang J, et al. Myeloid-derived suppressor cells participate in preventing graft rejection. Clinical & developmental immunology. 2012; 2012:731486. [PubMed: 22481970]
22. Hingorani SR, Petricoin EF, Maitra A, et al. Preinvasive and invasive ductal pancreatic cancer and its early detection in the mouse. Cancer Cell. 2003; 4:437–450. [PubMed: 14706336]
23. Hingorani SR, Wang L, Multani AS, et al. Trp53R172H and KrasG12D cooperate to promote chromosomal instability and widely metastatic pancreatic ductal adenocarcinoma in mice. Cancer Cell. 2005; 7:469–483. [PubMed: 15894267]
24. Hruban RH, Goggins M, Parsons J, et al. Progression model for pancreatic cancer. Clin Cancer Res. 2000; 6:2969–2972. [PubMed: 10955772]
25. Fleming TJ, Fleming ML, Malek TR. Selective expression of Ly-6G on myeloid lineage cells in mouse bone marrow. RB6-8C5 mAb to granulocyte-differentiation antigen (Gr-1) detects members of the Ly-6 family. J Immunol. 1993; 151:2399–2408. [PubMed: 8360469]
26. Geissmann F, Jung S, Littman DR. Blood monocytes consist of two principal subsets with distinct migratory properties. Immunity. 2003; 19:71–82. [PubMed: 12871640]
27. Nakano H, Yanagita M, Gunn MD. CD11c(+)B220(+)Gr-1(+) cells in mouse lymph nodes and spleen display characteristics of plasmacytoid dendritic cells. J Exp Med. 2001; 194:1171–1178. [PubMed: 11602645]
28. Palamara F, Meindl S, Holcmann M, et al. Identification and characterization of pDC-like cells in normal mouse skin and melanomas treated with imiquimod. J Immunol. 2004; 173:3051–3061. [PubMed: 15322165]
29. Matsuzaki J, Tsuji T, Chamoto K, et al. Successful elimination of memory-type CD8+ T cell subsets by the administration of anti-Gr-1 monoclonal antibody in vivo. Cell Immunol. 2003; 224:98–105. [PubMed: 14609575]
30. Peranzoni E, Zilio S, Marigo I, et al. Myeloid-derived suppressor cell heterogeneity and subset definition. Current opinion in immunology. 2010; 22:238–244. [PubMed: 20171075]
31. Geutskens SB, Otonkoski T, Pulkkinen MA, et al. Macrophages in the murine pancreas and their involvement in fetal endocrine development in vitro. J Leukoc Biol. 2005; 78:845–852. [PubMed: 16037409]

32. Fridlender ZG, Sun J, Mishalian I, et al. Transcriptomic analysis comparing tumor-associated neutrophils with granulocytic myeloid-derived suppressor cells and normal neutrophils. PLoS One. 2012; 7:e31524. [PubMed: 22348096]
33. Biermann H, Pietz B, Dreier R, et al. Murine leukocytes with ring-shaped nuclei include granulocytes, monocytes, and their precursors. J Leukoc Biol. 1999; 65:217–231. [PubMed: 10088605]
34. Hamilton JA. Colony-stimulating factors in inflammation and autoimmunity. Nat Rev Immunol. 2008; 8:533–544. [PubMed: 18551128]
35. Daley JM, Thomay AA, Connolly MD, et al. Use of Ly6G-specific monoclonal antibody to deplete neutrophils in mice. Journal of leukocyte biology. 2008; 83:64–70. [PubMed: 17884993]
36. Ribechini E, Leenen PJ, Lutz MB. Gr-1 antibody induces STAT signaling, macrophage marker expression and abrogation of myeloid-derived suppressor cell activity in BM cells. European journal of immunology. 2009; 39:3538–3551. [PubMed: 19830733]
37. Wolchok JD, Hoos A, O'Day S, et al. Guidelines for the evaluation of immune therapy activity in solid tumors: immune-related response criteria. Clinical cancer research : an official journal of the American Association for Cancer Research. 2009; 15:7412–7420. [PubMed: 19934295]
38. Ziegler SF, Ramsdell F, Alderson MR. The activation antigen CD69. Stem Cells. 1994; 12:456–465. [PubMed: 7804122]
39. Craston R, Koh M, Mc Dermott A, et al. Temporal dynamics of CD69 expression on lymphoid cells. J Immunol Methods. 1997; 209:37–45. [PubMed: 9448032]
40. Drake CG, Jaffee E, Pardoll DM. Mechanisms of immune evasion by tumors. Adv Immunol. 2006; 90:51–81. [PubMed: 16730261]
41. DuPage M, Cheung AF, Mazumdar C, et al. Endogenous T cell responses to antigens expressed in lung adenocarcinomas delay malignant tumor progression. Cancer Cell. 19:72–85. [PubMed: 21251614]
42. Willimsky G, Blankenstein T. Sporadic immunogenic tumours avoid destruction by inducing T-cell tolerance. Nature. 2005; 437:141–146. [PubMed: 16136144]
43. Stylianopoulos T, Martin JD, Chauhan VP, et al. Causes, consequences, and remedies for growth-induced solid stress in murine and human tumors. Proc Natl Acad Sci U S A. 2012; 109:15101–15108. [PubMed: 22932871]
44. Mahadevan D, Von Hoff DD. Tumor-stroma interactions in pancreatic ductal adenocarcinoma. Mol Cancer Ther. 2007; 6:1186–1197. [PubMed: 17406031]
45. Diaz-Montero CM, Salem ML, Nishimura MI, et al. Increased circulating myeloid-derived suppressor cells correlate with clinical cancer stage, metastatic tumor burden, and doxorubicin-cyclophosphamide chemotherapy. Cancer Immunol Immunother. 2009; 58:49–59. [PubMed: 18446337]
46. Montero AJ, Diaz-Montero CM, Kyriakopoulos CE, et al. Myeloid-derived suppressor cells in cancer patients: a clinical perspective. Journal of immunotherapy. 2012; 35:107–115. [PubMed: 22306898]
47. Porembka MR, Mitchem JB, Belt BA, et al. Pancreatic adenocarcinoma induces bone marrow mobilization of myeloid-derived suppressor cells which promote primary tumor growth. Cancer immunology, immunotherapy : CII. 2012
48. Brandau S, Trellakis S, Bruderek K, et al. Myeloid-derived suppressor cells in the peripheral blood of cancer patients contain a subset of immature neutrophils with impaired migratory properties. J Leukoc Biol. 2011; 89:311–317. [PubMed: 21106641]
49. Greten TF, Manns MP, Korangy F. Myeloid derived suppressor cells in human diseases. Int Immunopharmacol. 2011; 11:802–807. [PubMed: 21237299]
50. Goedegebuure P, Mitchem JB, Porembka MR, et al. Myeloid-derived suppressor cells: general characteristics and relevance to clinical management of pancreatic cancer. Current cancer drug targets. 2011; 11:734–751. [PubMed: 21599634]
51. Sanford DE, Belt BA, Panni RZ, et al. Inflammatory monocyte mobilization decreases patient survival in pancreatic cancer: a role for targeting the CCL2/CCR2 axis. Clin Cancer Res. 2013; 19:3404–3415. [PubMed: 23653148]

52. Gabrilovich DI, Ostrand-Rosenberg S, Bronte V. Coordinated regulation of myeloid cells by tumours. Nature reviews. Immunology. 2012; 12:253–268.

53. Iclozan C, Antonia S, Chiappori A, et al. Therapeutic regulation of myeloid-derived suppressor cells and immune response to cancer vaccine in patients with extensive stage small cell lung cancer. Cancer immunology, immunotherapy : CII. 2013; 62:909–918.

54. Puhalla S, Bhattacharya S, Davidson NE. Hematopoietic growth factors: personalization of risks and benefits. Molecular oncology. 2012; 6:237–241. [PubMed: 22497867]

SIGNIFICANCE OF THIS STUDY

What is already known about this subject?

- PDA is characterized by a robust desmoplastic reaction with multiple immune suppressive elements.
- T cell responses to antigens overexpressed by pancreas cancer can be detected and/or elicited in a substantial fraction of patients.
- Production of GM-CSF by PDA allografts or by preinvasive murine ductal cells enables the establishment and/or progression of transplantable tumor cell growth.[1, 2]

What are the new findings?

- Systemic and intratumoral accumulation of distinct subsets of immunosuppressive cancer-conditioned myeloid cells, each with their own kinetics, chronicles PDA progression.
- Primary and metastatic PDA cells secrete factors involved in the induction, recruitment and survival of myeloid cells leading to accumulation of MDSC.
- Targeted *in vivo* depletion of the Gr-MDSC subset resulted in a subsequent expansion of a distinct monocytic MDSC (Mo-MDSC) subset, yet was sufficient to induce the intratumoral accumulation of endogenous CD8 T cells and tumor cell apoptosis in autochthonous PDA.

How might it impact clinical practice in the foreseeable future?

- Modulation of cancer-conditioned myeloid cells may provide therapeutic benefit alone or in combination with other modalities. Successful translation of such strategies will benefit from in-depth investigation in rational models that reflect the natural pathobiology, antigenic diversity, and evolution of the cognate human disease.
- Developing strategies to target the plastic and interrelated myeloid cell lineages should take into account the potential for homeostatic regulation between distinct MDSC subsets.

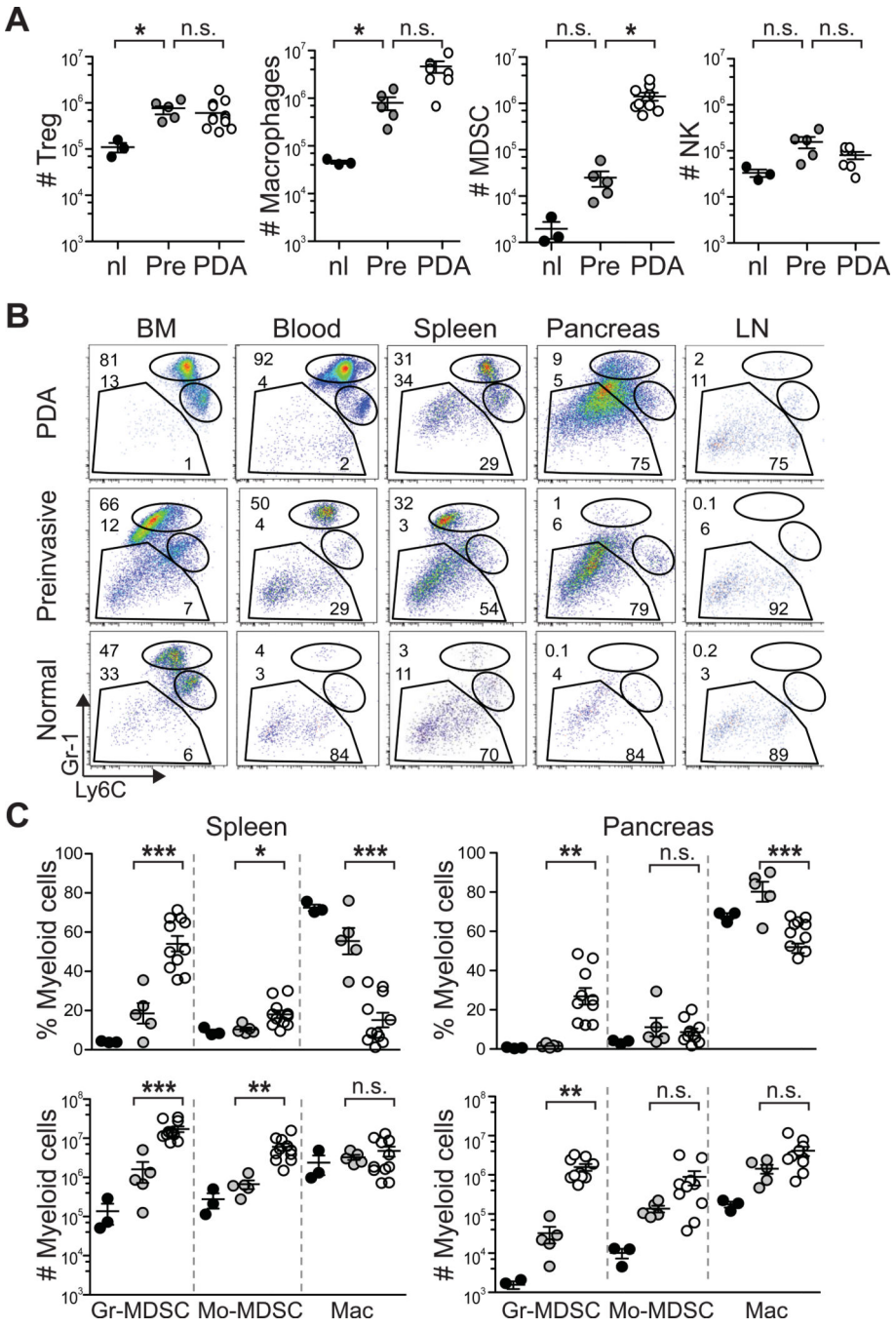

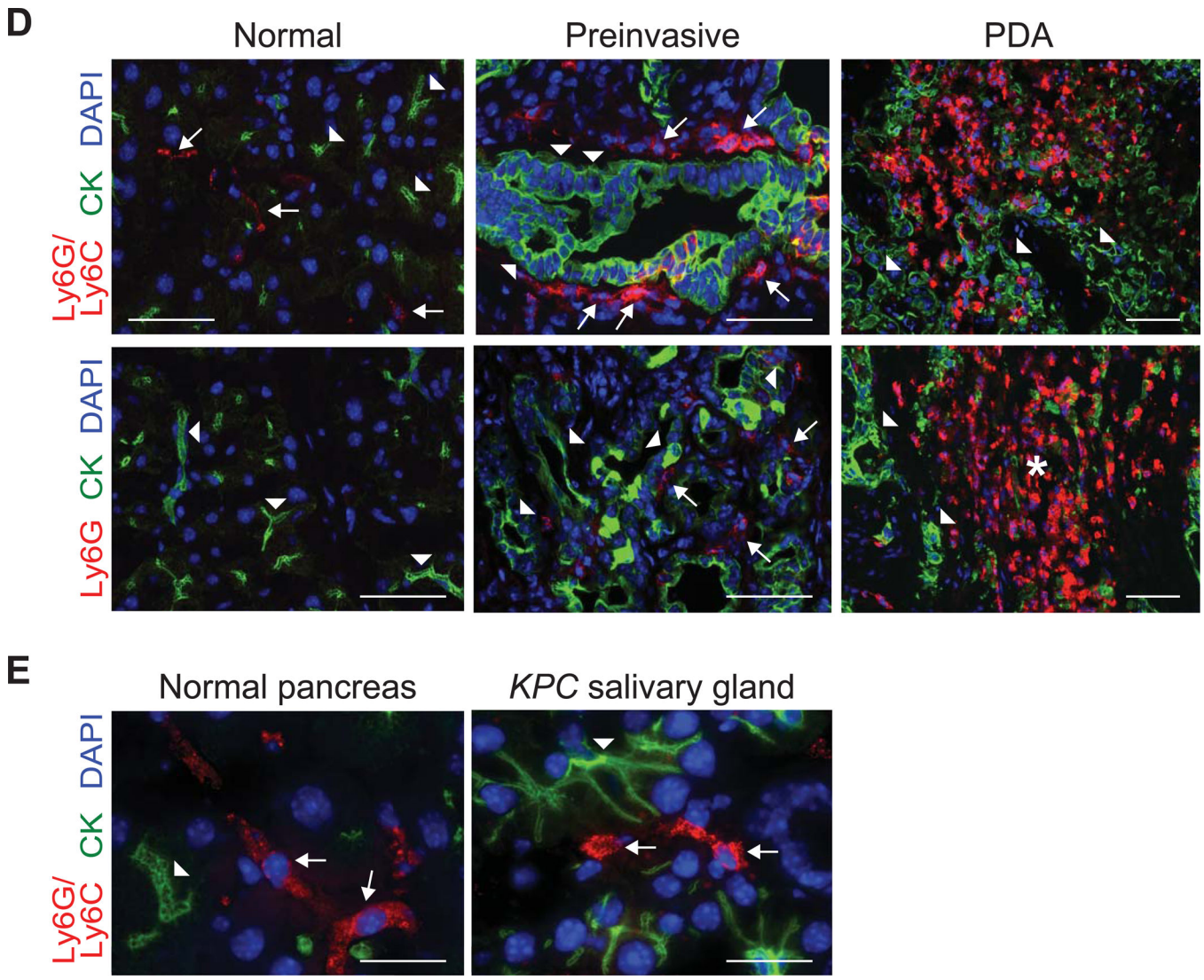

Figure 1.

Cancer-conditioned myeloid cells chronicle the evolution of PDA in *KPC* mice. (A) The number of pancreatic Treg ($CD45^+CD4^+FoxP3^+$), macrophages ($CD45^+CD11b^+F4/80^+$), MDSC ($CD45^+CD11b^+$RB6-8C5 [Ly6G/Ly6C]$^+$) and NK cells ($CD45^+NK1.1^+$) per pancreas were quantified from normal pancreas (nl), 6–8 week old *KPC* pancreata with confirmed preinvasive disease (Pre), and invasive tumors (PDA). Significant differences were detected in the number of Treg, TAM, and MDSC during disease progression. (B) Evolving profiles of three distinct populations of myeloid cells (gated on $CD45^+CD11b^+$) were observed in various organs based on expression patterns of Gr-1 and Ly6C. BM, bone marrow; LN, lymph node. (C) The percentages (top panel) and absolute numbers (bottom panel) of $CD45^+CD11b^+$ myeloid populations in the spleen and pancreas in normal (black filled circles) and preinvasive (gray filled circles) and invasive (open circles) disease settings. Data are plotted as mean ± SEM and each data point represents an individual mouse. Gr-MDSC = $CD45^+CD11b^+Gr\text{-}1^{high}Ly6C^{int}$; Mo-MDSC = $CD45^+CD11b^+Gr\text{-}1^{int}Ly6C^{high}$; and macrophage (Mac) = $CD45^+CD11b^+Ly6C^{int}$. (D)

Specific immunofluorescence reveals rare Ly6G/Ly6C$^+$ (RB6-8C5) cells in normal pancreas, focal accumulation in pancreata with preinvasive disease, and diffuse infiltration in invasive PDA. Specific Ly6G immunofluorescence demonstrates that Gr-MDSC are absent from normal pancreas, rare in preinvasive disease, and abundant in invasive PDA. The majority of myeloid cells in normal pancreas and surrounding preinvasive lesions appear to be macrophages. Arrowheads, epithelial cells; arrows, myeloid cells; asterisk, Gr-MDSC. Scale bars, 50 μm. (E) Ly6G/Ly6C (RB6-8C5) staining in normal pancreas and *KPC* salivary gland. Arrowheads, epithelial cells; arrows, myeloid cells. Scale bars, 10 μm. *, $p<0.05$; **, $p<0.005$; ***, $p<0.0005$.

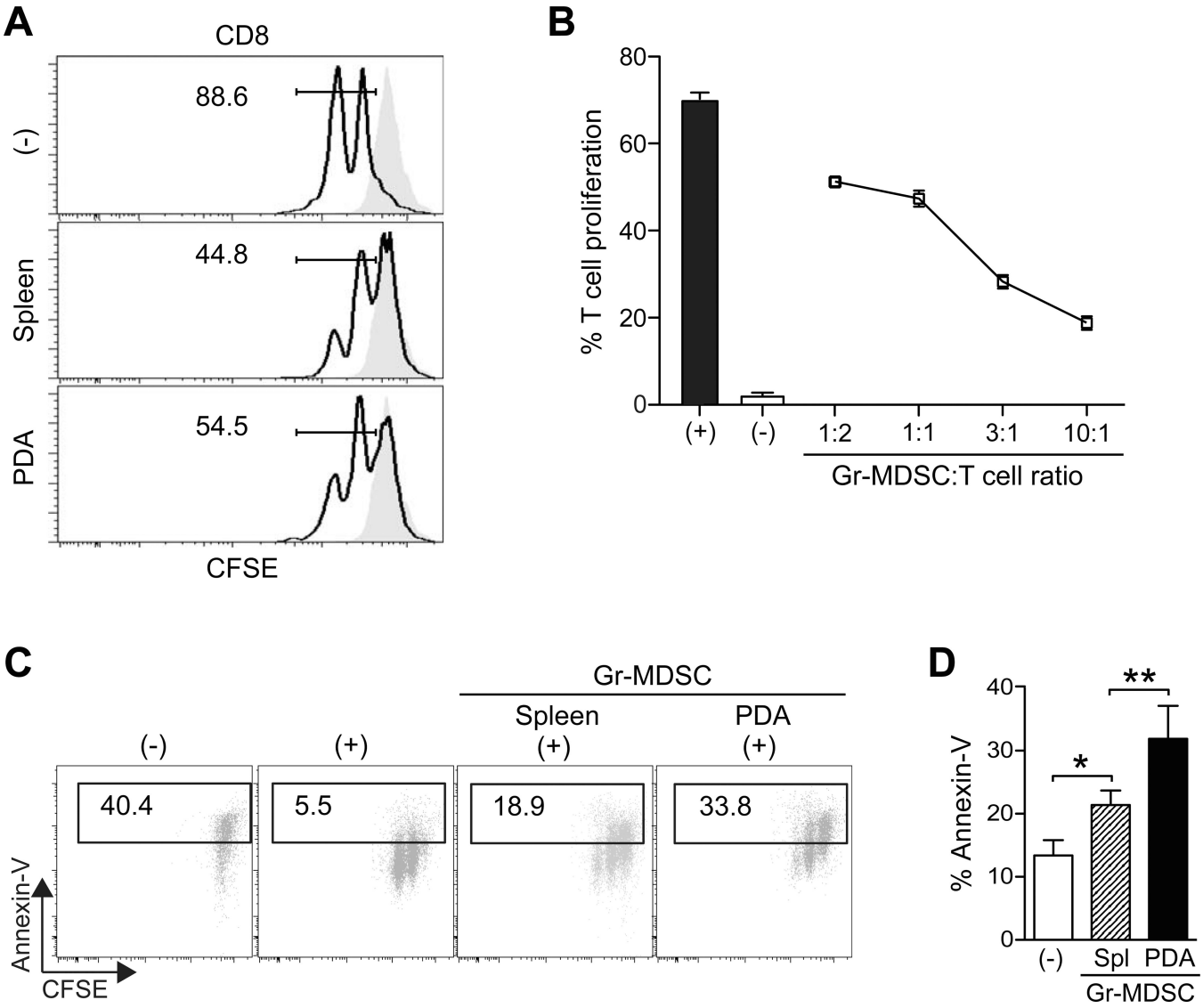

Figure 2.

Gr-MDSC isolated from the spleen and PDA are immunosuppressive. (A) Naïve T cell proliferation in response to anti-CD3/CD28 is suppressed by Gr-MDSC (assays performed at 1:1 Gr-MDSC:T cell ratio). Numbers indicate the percentage of CD8 T cells that have undergone ≥ 1 cell division after 48h. Gray filled histograms indicate T cells in the absence of CD3/CD28. (−) indicates no Gr-MDSC added. (B) The suppressive capacity of Gr-MDSC increases at higher Gr-MDSC:T cell ratios. Representative data from 1 of 4 independent experiments are plotted as mean ± SD (n=3 replicates each). (−) = no CD3/CD28 stimulation. (C) Gr-MDSC induce the apoptosis of activated T cells. Representative FACS profiles (of 4 independent experiments) performed at 1:1 Gr-MDSC:T cell ratio and gated on $CD8^+$ $Thy1.1^+$ cells. (−) = no stimulation; (+) = CD3/CD28 stimulation. (D) Gr-MDSC isolated from spleen (Spl) and PDA of *KPC* mice induce apoptosis of activated CD8 T cells. (−) = T cells only (no MDSC). Data represent mean ± SEM from 4 independent experiments.

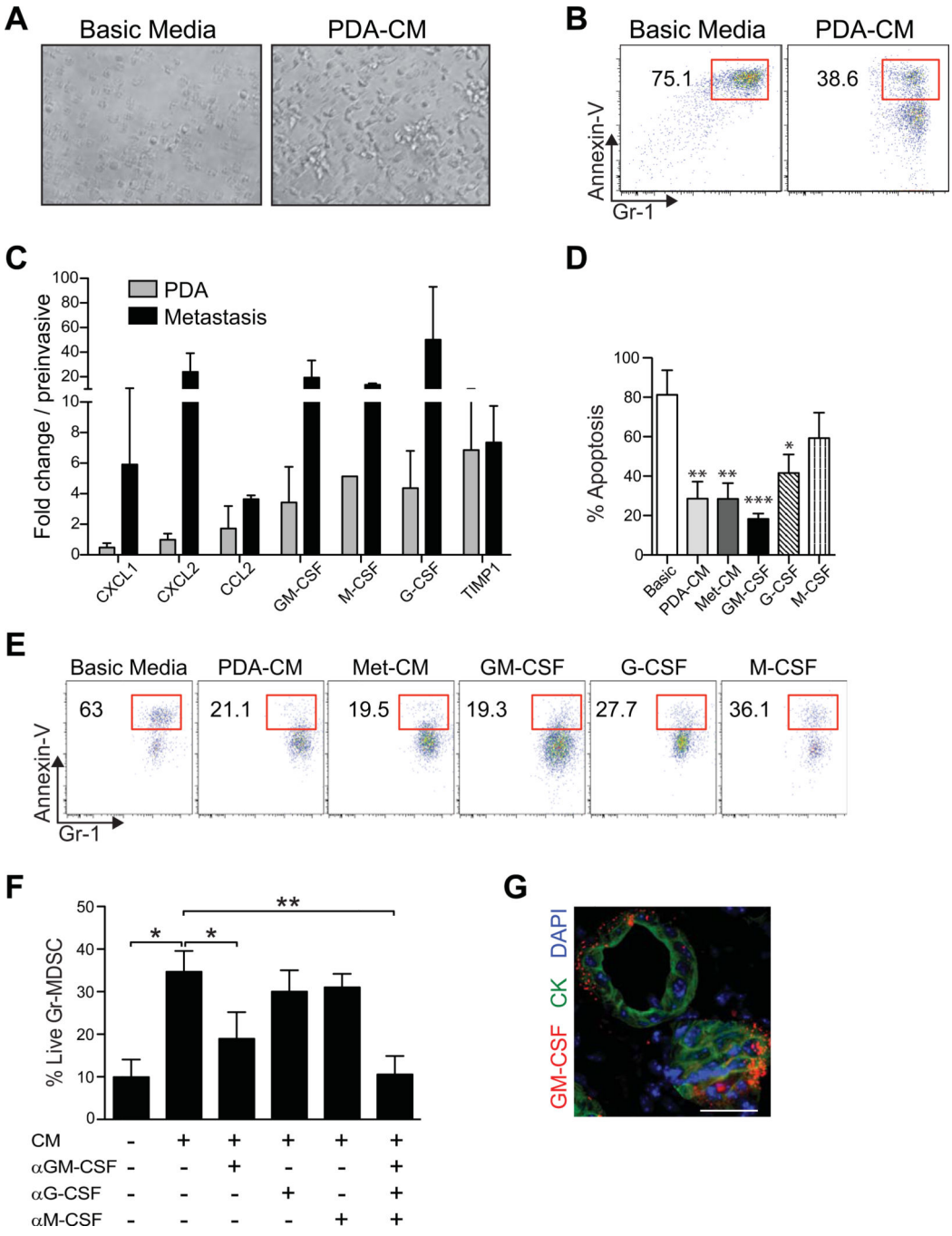

Figure 3.

Conditioned media from primary PDA (PDA-CM) or metastatic epithelial cells (Met-CM) promotes the survival of Gr-MDSC. (A) Sorted Gr-MDSC cultured in basic media or PDA-CM for 48h. (B) PDA-CM protects a cultured Gr-MDSC from apoptosis (48h). (C) Relative gene expression of select cytokines and chemokines as determined by quantitative PCR (data represent mean ± SEM of 3 independently derived primary invasive tumor (PDA) and paired metastatic cell preparations and are normalized to expression in preinvasive cells). (D) Impact of conditioned media and cytokines on apoptosis of splenic-derived Gr-MDSC.

Bar graphs represent mean ± SEM from 4 independent experiments performed. Treated samples were compared to the basic media (Basic) control and significance was determined by using a one-way ANOVA followed by a Dunnett's multiple comparison test. (E) Sorted splenic Gr-MDSC from *KPC* mice with PDA were incubated with the indicated media or cytokines and the percentage of Annexin-V^+ Gr-MDSC at 48h determined by FACS (representative results of 4 independent experiments). (F) Sorted splenic Gr-MDSC were incubated with PDA-CM ± the indicated blocking mAb for 48h. The percentage of live cells was determined by FACS analyses of Annexin-V^{neg} Gr-MDSC. (G) Clusters of PDA cells contain GM-CSF at their stromal surface. CK, cytokeratin. Scale bar, 25 μm. *, $p<0.05$; **, $p<0.005$; ***, $p<0.0005$.

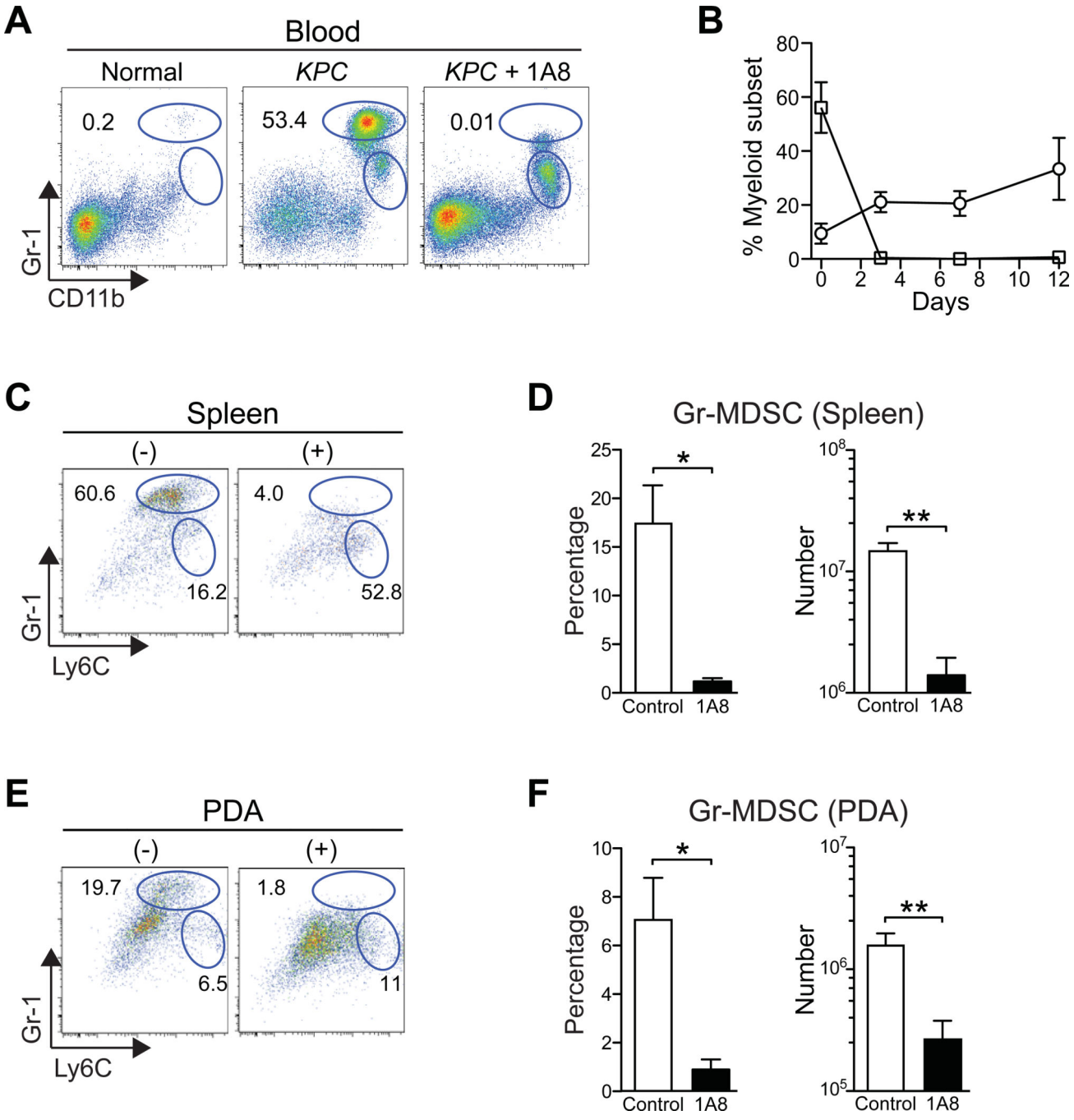

Figure 4.

Systemic administration of 1A8 (αLy6G) specifically depletes Gr-MDSC in autochthonous PDA. (A) Representative myeloid cell profiles in PBMC from a normal mouse and untreated (*KPC*) and 1A8-treated *KPC* (*KPC* + 1A8) mice. Numbers indicate the percentage of each subset gated on $CD45^+$ mononuclear cells. We note that the gates for the discrete subpopulations defined in the blood were then applied to the tissue-specific analyses. (B) Percentage of Gr-MDSC (squares) and Mo-MDSC (circles) in blood after 1A8 treatment. Data represent mean ± SD from n=3 independent treated animals. (C) Representative FACS

profiles of $CD45^+$ $CD11b^+$ splenocytes from control (−) and 1A8-treated (+) *KPC* mice (n=4–6 animals per group). (D) Both the percentage and number of splenic Gr-MDSC at endpoint of 1A8 treatment (day 12) are significantly decreased (**, p=0.005). (E) Representative FACS profiles of intratumoral myeloid cells in control (−) and 1A8-treated (+) *KPC* mice at day 12 of Gr-MDSC depletion. (F) The percentage and number of Gr-MDSC in PDA at endpoint are significantly decreased in 1A8-treated compared to control *KPC* mice.

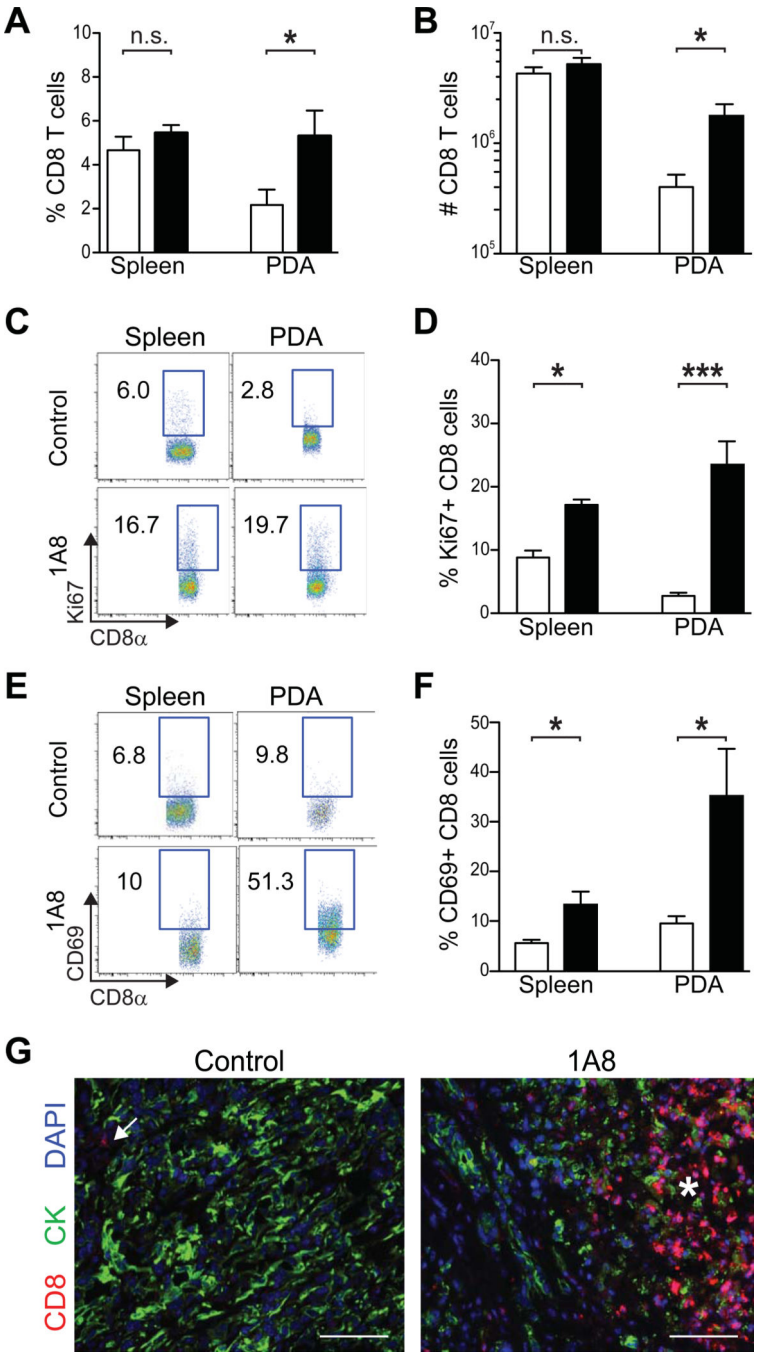

Figure 5.

Gr-MDSC depletion increases CD8 T cell number, proliferation, activation and tumor-specific infiltration in autochthonous PDA. The percentage (A) and number (B) of CD8 T cells significantly increased in pancreatic tumors, but not the spleen of 1A8-treated compared with untreated *KPC* mice. (C) Representative FACS plots of proliferating CD8 T cells in the spleen and pancreatic tumors of control and treated *KPC* mice as determined by Ki67 expression (n=4–6 mice per cohort). (D) The percentage of $Ki67^{+}$ CD8 T cells in 1A8-treated (n=4) compared to control *KPC* mice (n=6 mice) in the spleen and tumors was

significantly increased. (E, F) Gr-MDSC depletion increases the percentage of CD8 T cells in both the spleen and PDA that express the activation marker CD69. (G) CD8 T cells (arrow) are rare in control PDA and increase significantly (asterisk) after Gr-MDSC depletion (1A8). Control, open bars; 1A8-treated, filled bars. Scale bars, 50 μm.

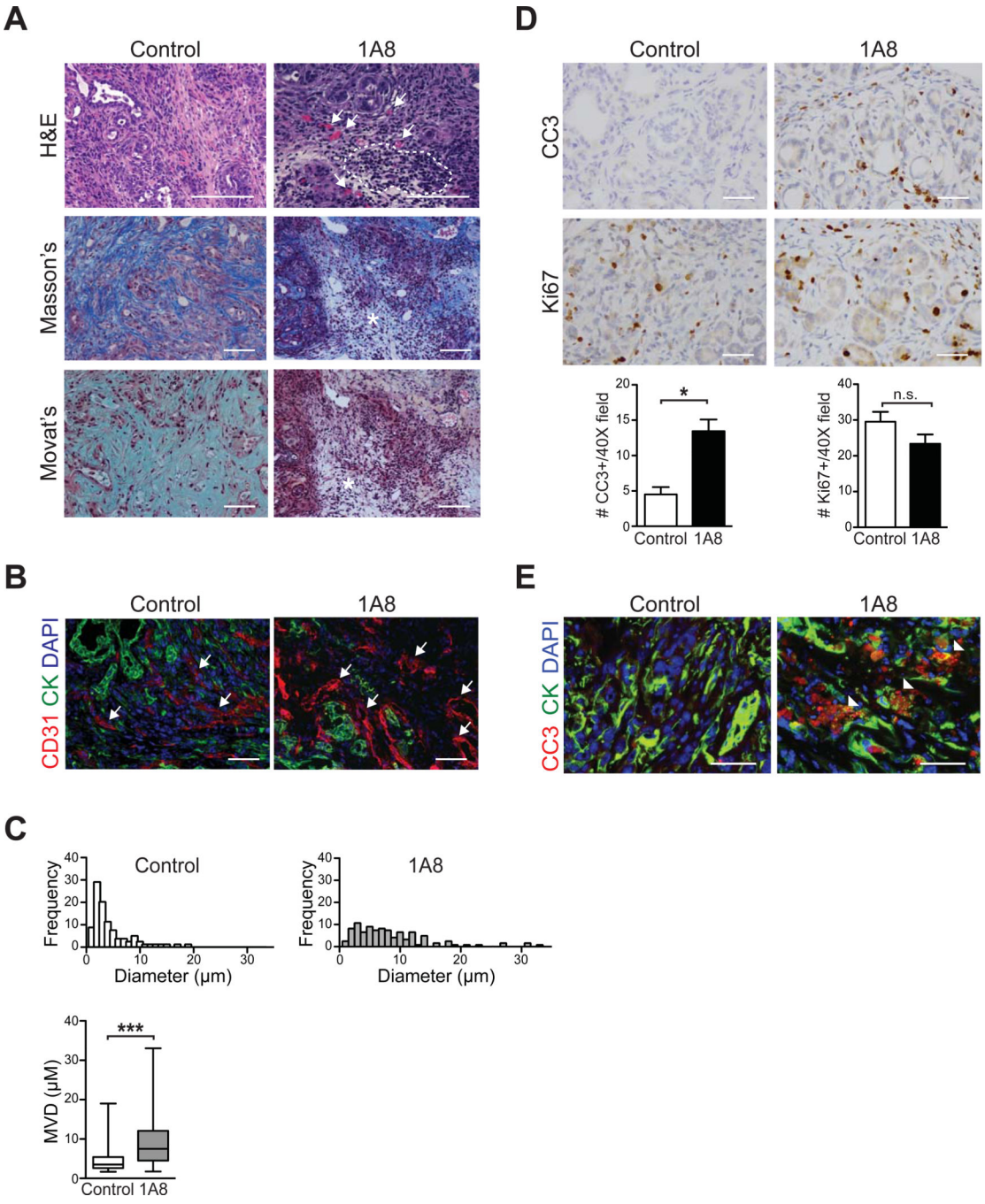

Figure 6.

Targeted depletion of Gr-MDSC remodels the stroma and increases tumor epithelial cell apoptosis. (A) Administration of 1A8 increases mononuclear cell infiltrates in autochthonous PDA (outlined) and patency of blood vessels (arrows), and depletes ECM content and integrity (asterisks). Representative fields are shown for histology (H&E), collagen content (Masson's trichrome) and combined collagen and glycosaminoglycan content (Movat's pentachrome). Scale bars, 50 μm. (B) CD31 immunofluorescence of PDA reveals a shift toward larger vessel diameters (arrows) after 1A8 treatment (quantified in

(C)). Scale bars, 25 μm. (C) Administration of 1A8 significantly increases the mean vessel diameter in PDA. (D) Apoptosis of tumor epithelial cells, as assessed by cleaved caspase-3 (CC3), was significantly increased in 1A8-treated (n=4) compared to control (n=6) *KPC* mice, while the number of proliferating tumor epithelial cells (Ki67) was not significantly different. (E) CC3 and CK double-positive cells indicate tumor epithelial cells undergoing apoptosis (arrowheads). Scale bars, 25 μm.